



Article

# Influence of Mutual Coupling on Stability of RCS Response in Chipless RFID

Jan Machac <sup>1,\*</sup> , Amine Boussada <sup>2</sup>, Milan Svanda <sup>1</sup>, Jaroslav Havlicek <sup>1</sup> and Milan Polivka <sup>1</sup>

<sup>1</sup> Department of Electromagnetic Field, Faculty of Electrical Engineering, Czech Technical University in Prague, 16627 Prague, Czech Republic; svandmil@fel.cvut.cz (M.S.); havlij18@fel.cvut.cz (J.H.); polivka@fel.cvut.cz (M.P.)

<sup>2</sup> Faculty of Engineering, University of Waterloo, Montreal, QC H3A 0E8, Canada; amineelmarsa@gmail.com

\* Correspondence: machac@fel.cvut.cz; Tel.: +420-224-352-279

Received: 31 May 2018; Accepted: 14 July 2018; Published: 17 July 2018



**Abstract:** The paper investigates the influence of mutual coupling between individual scatterings of chipless Radio Frequency Identification (RFID) tags based on its frequency-domain performance using a simplified equivalent circuit model. The proposed steady state analysis predicts a fast and satisfactory amplitude level and frequency position of resonant peaks of a predicted radar cross section (RCS) response. The proposed approach is capable of pre-evaluating a suitability of the particular scattered topology for implementing in chipless RFID tags. It is demonstrated on two different geometries.

**Keywords:** circuit model; chipless RFID; mutual coupling; RCS

## 1. Introduction

The most investigated chipless tag solutions are based on the frequency domain detection using the tag's specific spectral signature. These RFID tags are composed of arrays of small printed scatterers (coding particles). The principle of encoded information can be described as either presence or non-presence on each scatterer's peak in the tag's spectral signature, which represents logical one or zero, respectively [1]. These tags have been intensively investigated recently [1–7]. The aim is to find a microwave frequency equivalent of optical barcodes systems. The designed microwave tags must be, therefore, optimized with the aim to reduce the taken area. Reducing the distance between particular resonators, however, increases mutual coupling between them. Mutual coupling detunes the response of neighboring resonators in the tag. Due to this, the logical “zeros” that are coded by the absence of the corresponding resonance is difficult to detect since the neighboring resonances are detuned from their original position. This reduces and possibly prevents the reliability of reading the coded information. We have proposed two ways for reducing the mutual coupling. This includes increasing the distance between resonators by tapering their arms [8] and rearranging positions of resonators in the tag [9]. In this scenario, the resonators with neighboring resonant frequencies are located at a higher distance, which means their coupling is reduced.

Professional electromagnetic (EM) simulators usually require substantial time to perform full-wave analysis of resonator arrays and to calculate the radar cross section (RCS) or any equivalent quantity as a reflection coefficient in the plane of the RFID transponder. Equivalent electric circuits represent an effective tool for simplified and fast analysis of various microwave structures [10]. They reflect physical behavior of the structure and can accelerate preliminary analysis of originally very complex structures while sufficient or acceptable accuracy is maintained.

This paper employs a simple equivalent circuit model (ECM) (originally proposed in [11]) of the RFID tag composed of an array of U-folded dipoles [8,9] to predict and study its RCS

response. RCS at each frequency is related to currents flowing in individual coupled resonant circuits representing original tag scatterers. These currents correspond to the magnetic field of the reflected wave. The approach itself is subsequently applied toward understanding the influence of inter-element mutual coupling on the amplitude level and frequency stability of resonant peaks of predicted RCS response. This is crucial for proper identification of coded information by a chipless tag.

The paper further compares predicted and measured RCS response of the tag composed of U-folded dipoles presented in Reference [1] with recently proposed tapered U-folded dipoles [8] and with the tag composed of resonators rearranged in their positions [9]. Based on that evidence, the advantage of the tags with reduced mutual coupling between neighboring resonators is shown.

Therefore, the proposed simplified analysis might serve to pre-evaluate the suitability of particularly shaped scatterers that are intended to be used to implement chipless RFID tags. Results obtained by the equivalent circuit modeling and measurement exhibit satisfactory agreement.

## 2. Tags with Reduced Inter Element Coupling

The geometry of the recently proposed uniplanar strip scatterer with tapered arms [8] was originally inspired by the U-folded dipole presented in Reference [1]. All scatterers were designed on the low loss substrate Rogers RO4003 ( $\epsilon_r = 3.38$ ,  $\tan\delta = 0.002$ ) of the thickness 0.2 mm. The resonant frequencies were selected around 2.6 GHz depending on their length. Figure 1a shows the original U-folded dipole (UD) that has the outer size  $20 \times 2.5$  mm with the strip width 1 mm and the gap size 0.5 mm in accordance with Reference [1]. The tapered U-folded dipole (T-UD) of the same outer size is depicted in Figure 1b. The strip is 0.25 mm in width and the gap at the open end between the arms is 0.5 mm wide.

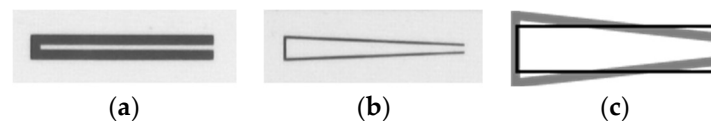


**Figure 1.** Layouts of investigated modifications of folded-dipole scatterers. (a) U-folded dipole (UD). (b) Tapered U-folded dipole (T-UD). (c) Approximation of the T-UD by a rectangular loop.

Another way to reduce the mutual coupling between planar resonators has been obtained by using an array with rearranged positions of resonators [9]. Tags with rearranged positions of resonators are shown in Figure 2c. The width of arms is 1 mm.

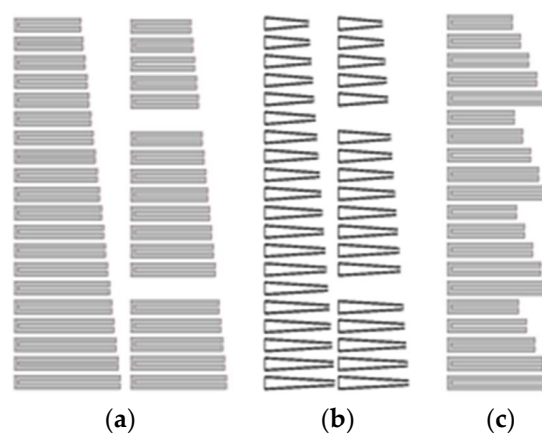


**Figure 2.** Layouts of investigated modifications of folded-dipole scatterers arrays. (a) 20-element arrays [1] coding information 111111111111111111, and 1111101111111011111 by missing 6th and 15th elements, (b) arrays of 20 T-UDs [8], (c) rearranged resonators in the array [9] coding the same information.

### 3. Equivalent Circuit Model of Resonator Array

Figure 2b shows the layout of the uni-planar RFID chipless tag composed of an array of 20 T-UDs presented in Reference [8]. The equivalent circuit of the  $i$ th single resonator is composed of a series resonant circuit  $L_i$ ,  $C_i$ , and  $R_i$  (see Figure 3) [11]. This circuit is fed by the source of voltage  $V_i$  that corresponds to the incident electric field  $E$  irradiating the tag.

$$V_i = E l_{i\text{eff}} \quad (1)$$

where  $l_{i\text{eff}}$  is the effective length of the  $i$ th resonator working as a receiving antenna. Changing amplitudes and phases of  $V_i$ , we can simulate oblique incidence of the wave or its different forms-planar, cylindrical, and spherical. The presented analysis is done for the perpendicular incidence of the plane wave so all voltages are taken  $V_i = 1$  and are in-phase. The magnetic field of the reflected wave excited by dipoles corresponds linearly to the current flow along these dipoles [12]. Predicted RCS is, therefore, proportional to the power of the sum of currents and, in particular, resonators of the equivalent circuit [13].

$$\text{RCS} \sim \left( \sum_{i=1}^{20} I_i \right)^2 \quad (2)$$

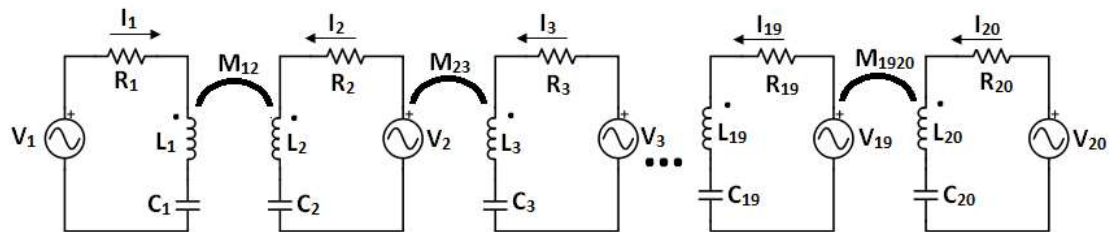


Figure 3. Equivalent circuit of the tag composed of 20 resonant elements.

The particular resonant circuits are coupled by a magnetic field and this coupling is represented by mutual inductances. The coupling coefficient decreases with increasing distances, which is shown in Figure 4. Consequently, it is sufficient to consider only coupling of the neighboring resonators. This has been proven by analyzing the circuit from Figure 3 by adding mutual inductances between the second neighbors.

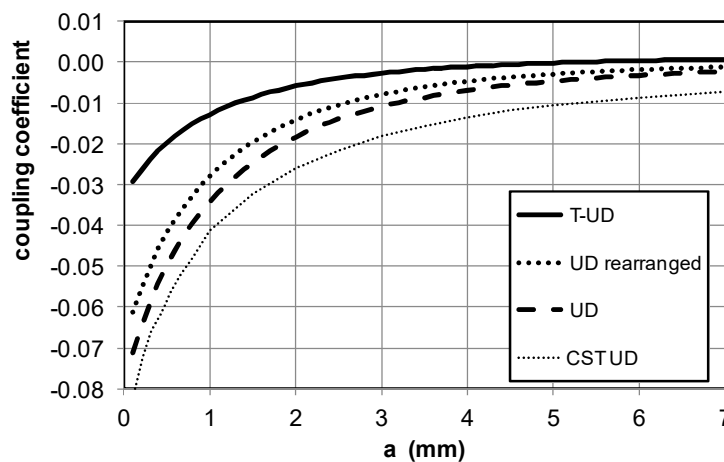


Figure 4. Coupling coefficient of adjacent pairs of original UD [1], T-UDs [8], and rearranged UD [9].

The missing resonator in the tag codes bit with logical '0' is represented by a circuit with resistance  $R_i = 1 \text{ M}\Omega$  that assures nearly a zero value of the passing current and consequently no (or negligible) contribution to the response (2). Equations for each loop in the circuit from Figure 3 are shown below.

$$\left. \begin{aligned} -V_1 + (R_1 + X_{L1} + X_{C1})I_1 + X_{M12}I_2 &= 0 \\ -V_2 + (R_2 + X_{L2} + X_{C2})I_2 + X_{M12}I_1 + X_{M23}I_3 &= 0 \\ &\dots\dots \\ -V_{19} + (R_{19} + X_{L19} + X_{C19})I_{19} + X_{M1819}I_{18} + X_{M1920}I_{20} &= 0 \\ -V_{20} + (R_{20} + X_{L20} + X_{C20})I_{20} + X_{M1920}I_{19} &= 0 \end{aligned} \right\} \quad (3)$$

where  $X_{Li} = j\omega L_i$ ,  $X_{Mij} = j\omega M_{ij}$ , and  $X_{Ci} = 1/(j\omega C_i)$ . Solution of (3) determines the particular currents and the tag RCS response (2).

#### 4. Calculation of Dipole Inductances and Mutual Inductances

The folded dipoles shown in Figure 1a,b can be viewed as current loops and their inductance and mutual inductance of a pair of the loops can be calculated by using Neumann's formula from Reference [12].

$$M = \frac{\mu_0}{4\pi} \iint \frac{dl_1 \cdot dl_2}{|r_{12}|} \quad (4)$$

In Equation (4),  $dl_1$  and  $dl_2$  are elements of the loops and  $r_{12}$  is the oriented distance between these elements. To simplify the calculation, the original folded dipole is substituted by the current loop located at the inner edges of strips. The tapered U-folded dipole is substituted by the rectangular current loop, which is drawn in Figure 1c. The distribution of current passing along the dipoles arms described by the sine function is approximated by an average value equal to  $2/\pi$ .

The coupling coefficient that describes the mutual inductance between the pair of elements with inductances  $L_1$  and  $L_2$  and mutual inductance  $M$  is defined by the equation below.

$$\kappa = M / \sqrt{L_1 L_2} \quad (5)$$

The coupling coefficient of adjacent pairs of UDs, T-UDs, and rearranged UDs, 25 mm, and 25.5 mm in length, located at distance  $a$ , is plotted in Figure 4. The mutual coupling of T-UDs is significantly weaker than the coupling between UDs. This documents the basic advantage of the proposed tapered U-folded dipoles. Another way to reduce the mutual inter element coupling is to use the array with rearranged resonator positions [9]. The effect of the reduced coupling coefficient is not apparent here (Figure 4).

Figure 4 further shows the line marked CST UD, which represents the transmission between two UDs calculated by the CST Microwave Studio. The two resonators are fed by point ports connected to the open end. This verifies the behavior described above.

#### 5. Analysis Results

The results of the equivalent circuit analysis (RCS) are normalized. This occurs when values of all exciting voltages are equal to 1 V. The other source of inexact results follows from a rough estimate of RCS calculated by Equation (2).

The equivalent circuit analysis was applied to evaluate performance of up to 20-element arrays of proposed T-UD sequentially detuned by changing their length by 0.5 mm from 16 mm to 25.5 mm so that the outer size of the array is  $69 \times 25.5 \text{ mm}^2$  (see Figure 2b). RCS of fabricated tags was measured by a one-port vector measurement of monostatic RCS in a free space [8]. The obtained results were verified by simulations performed using the Zeland IE3D software (Mentor Graphics, Wilsonville, OR, USA).

The circuit parameters in the equivalent circuit were determined by calculating data for Figure 4. Capacitances were calculated from resonant frequencies of particular resonators and their inductances. Resistor values were evaluated using the skin effect [12].

$$R_i = l_i / (\sigma 2\delta w) \quad (6)$$

where  $l_i$  is total length of the strip  $w$  in width,  $\sigma$  is conductivity, and  $\delta$  is the penetration depth.

The first analyzed structure is one from Figure 2a. There is no measure taken here to reduce the coupling. Figure 5 shows the response of the tag composed of 18-element and 20-element UDs from Figure 1a. The resonators are coupled relatively strongly. The exceptions are the first and last resonators. They have neighbors from only one side so RCS at maximum of the first resonator response is higher than in the case of others. RCS at maximum of the last resonator is lower. The solid line shows a response of the tag with particular UD resonators removed to code logical zero bit information. Peaks adjacent to missing resonances are strongly distorted both in the amplitude level and the frequency position. Strong element coupling, therefore, makes the coded information difficult to read properly and predicts that such elements are not suitable for implementing in chipless RFID tags.

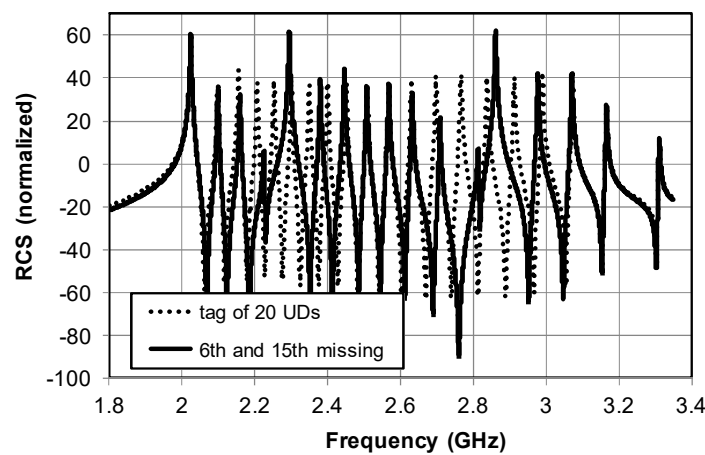


**Figure 5.** Predicted RCS response of the equivalent circuit of 20-element tag composed of U-folded dipoles [1] compared with the 18-element version coded by missing the 6th and 15th elements.

Yet, weak mutual coupling in the case of an array of recently proposed T-UD resonators of Figure 1b presented in Reference [8] assures a stable amplitude level and frequency positions of adjacent resonant peaks. Consequently, it enables their reliable identification in comparison with the RCS response of the full 20-bit tag (see Figure 6). Table 1 lists parameters of the equivalent circuit used to analyze the tag from Figure 2b.

**Table 1.** Elements of the equivalent circuit from Figure 4 used to calculate RCS of the tag from Figure 2b, which are presented in Figure 6.

$i$	$f_{oi}$ (GHz)	$l_i$ (mm)	$L_i$ (nH)	$i$	$R_i$ ( $\Omega$ )
1	2.074	25.5	16	−0.024	0.3
2	2.110	25	15.7	−0.0238	0.295
3	2.159	24.5	15.4	−0.0236	0.29
4	2.200	24	15.1	−0.0234	0.285
5	2.252	23.5	14.8	−0.0232	0.28
6	2.296	23	14.5	−0.023	0.275
7	2.342	22.5	14.2	−0.0228	0.27

Table 1. Cont.

$i$	$f_{oi}$ (GHz)	$l_i$ (mm)	$L_i$ (nH)	$i$	$R_i$ ( $\Omega$ )
8	2.390	22	13.9	-0.0226	0.265
9	2.447	21.5	13.6	-0.0224	0.26
10	2.500	21	13.3	-0.0222	0.255
11	2.559	20.5	13	-0.022	0.25
12	2.624	20	12.7	-0.0218	0.245
13	2.692	19.5	12.4	-0.0216	0.24
14	2.763	19	12.1	-0.0214	0.235
15	2.833	18.5	11.8	-0.0212	0.23
16	2.903	18	11.5	-0.021	0.225
17	2.985	17.5	11.2	-0.0208	0.22
18	3.067	17	10.9	-0.0206	0.215
19	3.157	16.5	10.6	-0.0204	0.21
20	3.254	16	10.3	-0.0202	0.205

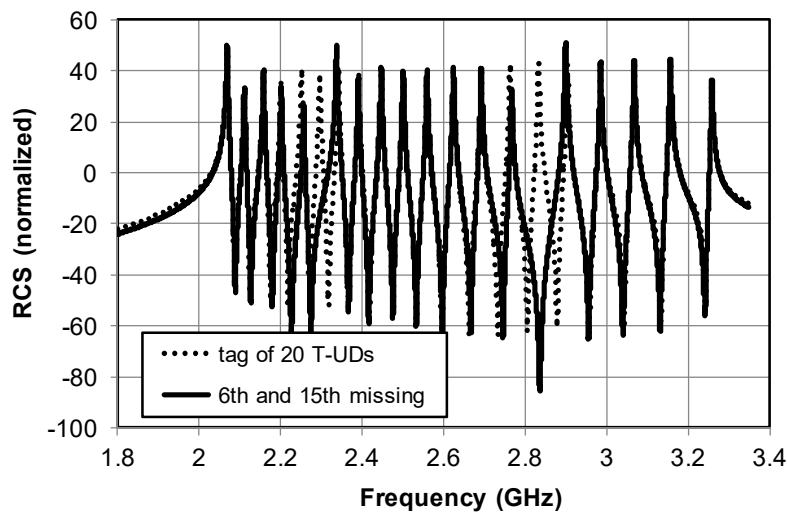


**Figure 6.** Predicted RCS response for the equivalent circuit of 20-element tag composed of tapered U-folded dipoles from Figure 2b compared with the 18-element version coded by missing the 6th and 15th elements.

Verification of the simulated results was performed by the monostatic measurement of tags RCS performance by an R & S ZVA 40 network analyzer in frequency band 2 to 4 GHz in an anechoic chamber (see Figure 7). It was based on the reflection coefficient evaluation of the double ridge horn antenna DRH 20 [14] in front of which a scatterer at a distance of 150 mm was placed. The tag's RCS response was calculated with the help of the relation used in Reference [1] and modified so that it was applicable to the one-port case described in Reference [9].

$$\sigma^{tag} = \left( \frac{S_{11}^{tag} - S_{11}^{iso}}{S_{11}^{ref} - S_{11}^{iso}} \right)^2 \sigma^{ref} \quad (7)$$

where  $S_{11}^{tag}$  is the reflection coefficient when the measured tag is used as a scatterer.  $S_{11}^{ref}$  represents the reflection coefficient when the reference plate is used as a scatterer.  $S_{11}^{iso}$  is the reflection coefficient of the antenna in case no scatterer is used and comprises the residual reflection from the experimental surroundings.  $S_{11}^{tag}$  is the RCS of the measured tag and  $\sigma^{ref}$  is the RCS of the reference scatterer, which is

the rectangular metal plate  $25 \times 70 \text{ mm}^2$  in size (corresponding with the measured tags) and 0.3 mm in thickness. Its analytical formula for RCS is shown below.

$$\sigma^{ref} = 4\pi \frac{a^2 b^2}{\lambda^2} \quad (8)$$

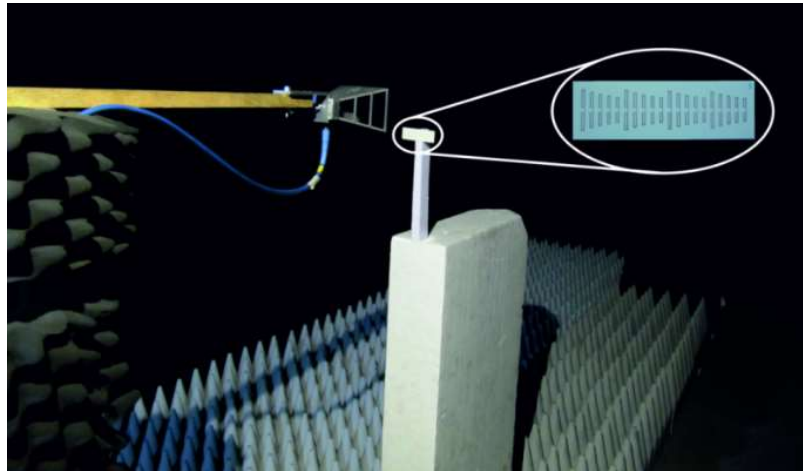


**Figure 7.** Monostatic measurement configuration in an anechoic chamber.

The monostatic measurement arrangement enables the avoidance of the use of angular dependent formula for reference scatterer and eliminates the influence of mutual coupling of the transmitting and receiving antennas in case of bi-static measurement.

The measurement received that power  $P_R$  can be determined using the well-known radar equation [15].

$$P_R = \frac{\sigma^{tag} \lambda^2 G^2}{(4\pi)^3 r^4} P_T \quad (9)$$

where  $r$  is a distance between the antenna and the tag with RCS equal to  $\sigma^{tag}$  and VNA transmitted power  $P_T$  equals 10 dBm and gain of the transmitted/received antenna  $G$  is 8 dBi. The received power for a measurement distance  $r = 150 \text{ mm}$  is calculated as approximately  $-52 \text{ dBm}$  for the frequency band center, which is valuable with a sufficient reserve in comparison with the noise threshold of the VNA or another receiving device. However, a relatively low measurement distance  $r$  was used because the guarantee is significantly higher than the reflection from the measured tag in comparison with a number of residual reflections from experimental surroundings. Consequently, clear RCS response can be evaluated from this measurement, according to Reference [7].

In spite of the expected smaller range, this solution can be suitable for certain chipless RFID applications operated on a short distance, e.g., identification of small objects on a transport belt, etc.

The results of the equivalent circuit analysis plotted in Figure 6 can be well compared with experimental data presented in Reference [8]. Figure 8 shows measured RCS response of the T-UD tags composed of 20 and 18 resonators. What cannot be exactly compared is the level of the RCS response. The RCS calculated from the equivalent circuit represents only some normalized values since all voltages are taken equal to 1 regardless of dipole effective lengths and RCS values are substituted by the sum of currents (2). Predicted RCS shown in Figure 6 and measured in Figure 8 proves the suitability of the structure, i.e., recognition of individual resonances from Figure 2b to design the RFID tag.

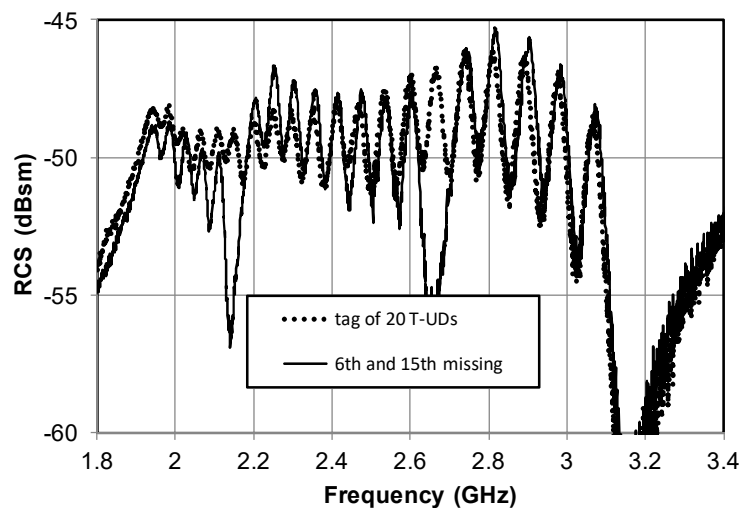


**Figure 8.** Measured RCS response of 20-element tags composed of tapered U-folded dipoles and tag coded by missing the 6th and 15th elements [8].

The coupling coefficient between two T-UD resonators (Figure 2b) at their distance equal to 1 mm is  $-0.013$ . This is a sufficiently low value that assures reliable reading of the coded information (see Figures 6 and 8). To get the same behavior of the tag composed of UD (Figure 2a), the distance between resonators must be increased to 2.7 mm. Therefore, the size of the chip would be significantly increased.

Another way to reduce the mutual coupling in arrays of planar resonators was proposed in Reference [9]. The positions of resonators in the array are rearranged according Figure 2c. Figure 9 plots RCS of this tag calculated with the help of the equivalent circuit. It is possible to distinguish reliably the missing resonances of the missing resonant elements. The amplitudes and frequency positions of adjacent resonant peaks are not affected. The plot documents the suitability of that simple solution to predict the tag behaviors documented by measured RCS plotted in Figure 10.

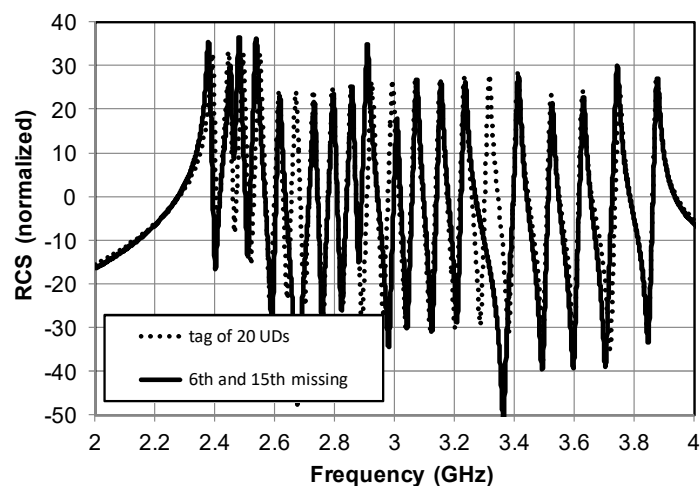


**Figure 9.** RCS response of the equivalent circuit of 20-element tag with rearranged resonators [9] compared with the 18-element version coded by the missing 6th and 15th elements from Figure 2b.

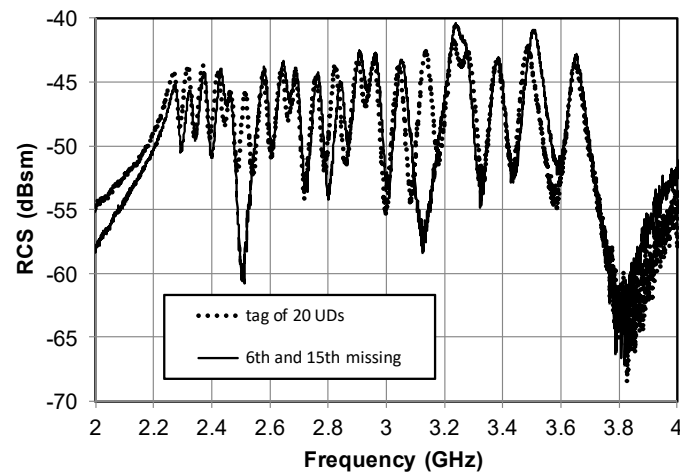


**Figure 10.** Measured RCS response of a 20-element tag with rearranged resonators and an 18-element tag coded by the missing 6th and 15th elements from Figure 2c [9].

Measurement results of both tags with reduced mutual coupling can be compared with the measured RCS response of the original tag without any measure taken to reduce the coupling plotted in Figure 11. The calculated response of this tag is plotted in Figure 5.

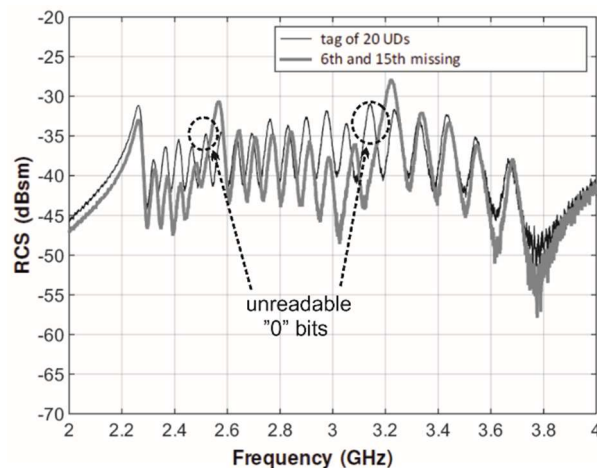


**Figure 11.** Measured RCS response of the 20-element tag composed of U-folded dipoles [1] compared with the 18-element version coded by the missing 6th and 15th elements.

## 6. Conclusions

We investigated the influence of mutual coupling between individual scatterers of chipless RFID tag on its frequency-domain performance. The RCS response was determined by a simplified equivalent circuit model. However, the proposed steady state analysis is, in fact, simple since it predicts the amplitude level and frequency positions of resonant peaks of predicted RCS, which respond quickly and effectively. This is a very fast and efficient tool that is capable of pre-evaluating a suitability of the particular scatterers for implementing in the chipless RFID tags.

We confirmed that using this simplified approach for topology modification of original U-folded scatterers or rearrangement of their position in a scatterer array reduces mutual coupling and improves amplitude and frequency stability of its RCS response, which is crucial for reliable reading of coded information in chipless RFID tags. The problem is in reading logical zeros. The coded logical zero is represented in the investigated tags by the “missing” resonator that is realized by setting very high resistance (1 M $\Omega$ ). Currently, in the case of the tag with the strongly coupled resonators, this strong

inter-element mutual coupling causes significant distortion of the amplitude level and frequency positions of adjacent resonant peaks of the RCS curve (see Figure 5). Such behavior makes it difficult to read the coded information. This predicts that such elements are not good candidates for scatterers. We advise to use scatterers with reduced mutual coupling and/or rearrange the scatterers in the array in such a way that frequency adjacent resonators are placed further apart to reduce coupling. This has been proven by analyzing tag composed resonators in the shape of tapered folded dipoles. The taper effectively increases the distance between resonators [8]. The tag with rearranged resonators [9] was analyzed and the concept of reducing the mutual coupling to improve the reading reliability was proven.

**Author Contributions:** J.M., M.S. and M.P. conceived and designed the experiments and analysed the data. M.S. and J.H. performed the experiments. A.B. and J.H. performed the model implementation. J.M. wrote the paper.

**Funding:** This research was funded by the Czech Science Foundation grant number GA17-00607S (analysis and simulations) and GA17-02760S (experiments).

**Conflicts of Interest:** The authors declare no conflict of interest.

## References

1. Vena, A.; Perret, E.; Tedjini, S. A Fully Printable Chipless RFID Tag with Detuning Correction Technique. *IEEE Microw. Wirel. Compon. Lett.* **2012**, *22*, 209–211. [CrossRef]
2. Polivka, M.; Svanda, M.; Machac, J. Chipless RFID Tag with an Improved RCS Response. In Proceedings of the 44th European Microwave Conference, Roma, Italy, 6–9 October 2014; pp. 770–773.
3. Vena, A.; Perret, E.; Tedjini, S. Design of Compact and Auto-Compensated Single-Layer Chipless RFID Tag. *IEEE Trans. Microw. Theory Tech.* **2012**, *60*, 2913–2924. [CrossRef]
4. Amin, E.M.; Bhuiyan, M.S.; Karmakar, N.C.; Winther-Jensen, B. Development of a Low Cost Printable Chipless RFID Humidity Sensor. *IEEE Sens. J.* **2014**, *14*, 140–148. [CrossRef]
5. Vena, A.; Perret, E.; Tedjini, S. High-Capacity Chipless RFID Tag Insensitive to the Polarization. *IEEE Trans. Antennas Propag.* **2012**, *60*, 4509–4515. [CrossRef]
6. Rezaiesarlak, R.; Manteghi, M. Complex-Natural-Resonance-Based Design of Chipless RFID Tag for High-Density Data. *IEEE Trans. Antennas Propag.* **2014**, *62*, 898–904. [CrossRef]
7. Feng, C.; Zhang, W.; Li, L.; Han, L.; Chen, X.; Ma, R. Angle-Based Chipless RFID Tag with High Capacity and Insensitivity to Polarization. *IEEE Trans. Antennas Propag.* **2015**, *63*, 1789–1797. [CrossRef]
8. Machac, J.; Polivka, M.; Svanda, M.; Havlicek, J. Reducing Mutual Coupling in Chipless RFID Tags Composed of U-Folded Dipole Scatterers. *Microw. Opt. Technol. Lett.* **2016**, *58*, 2723–2725. [CrossRef]
9. Polivka, M.; Havlicek, J.; Svanda, M.; Machac, J. Improvement in Robustness and Recognizability of RCS Response of U-Shaped Strip-Based Chipless RFID Tags. *IEEE Antennas Wirel. Propag. Lett.* **2016**, *15*, 2000–2003. [CrossRef]
10. Machac, J.; Mesa, F. Revisiting equivalent circuit models for emerging technologies: From microwaves to THz. In Proceedings of the Workshop WFA, International Microwave Symposium, Tampa Bay, FL, USA, 1–6 June 2014.
11. Boussada, A.; Machac, J.; Svanda, M.; Havlicek, J.; Polivka, M. Erroneous Reading of Information in Chipless RFID Tags. In Proceedings of the 2017 Progress in Electromagnetics Research Symposium—Spring (PIERS) 2017, St. Petersburg, Russia, 22–25 May 2017.
12. Jackson, J.D. *Classical Electrodynamics*, 3rd ed.; John Wiley & Sons: Hoboken, NJ, USA, 1999.
13. Huynen, J.H. *Phenomenological Theory of Radar Targets, Electromagnetic Scattering*, 1st ed.; Uslenghi, L.E., Ed.; Academic Press: New York, NY, USA, 1978.
14. RFspin. Model DRH20—Double Ridge Waveguide Horn. Available online: <http://www.rfspin.cz/en/antennas/drh20.php> (accessed on 16 July 2018).
15. Balanis, C.A. *Antenna Theory Analysis and Design*, 2nd ed.; John Wiley & Sons: Hoboken, NJ, USA, 1997.

